Enhanced adsorption and slow release of phosphate by dolomite–alginate composite beads as potential fertilizer

Yu-Xi Huang,[1,2] (iD) Meng-Jie Liu,[3] Shi Chen,[3] Irfan Iskandar Jasmi,[2] Yuanzhi Tang,[4] Shihong Lin[2,5]

[1]School of Environmental Science and Engineering, Sun Yat-sen University, Guangzhou, China

[2]Department of Civil and Environmental Engineering, Vanderbilt University, Nashville, Tennessee

[3]School of Environmental Science & Engineering, Huazhong University of Science and Technology, Wuhan, China

[4]School of Earth and Atmospheric Sciences, Georgia Institute of Technology, Atlanta, Georgia

[5]Department of Chemical and Biomolecular Engineering, Vanderbilt University, Nashville, Tennessee

• **Abstract**

The recovery and reuse of phosphorus (P) from wastewater treatment process is a critical and viable target for sustainable P utilization. This study explores a novel approach of integrating ultrafine mineral particles into hydrogel matrixes for enhancing the capacity of phosphate adsorption. Dolomite-alginate (DA) hydrogel beads were prepared by integrating ball-milled, ultrafine dolomite powders into calcium cross-linked alginate hydrogel matrix. The adsorption isotherms followed a Langmuir–Freundlich adsorption model with higher specific adsorption capacity than those reported in literature. The kinetics of phosphate adsorption suggest that the adsorption is diffusion controlled. Investigation of adsorption capacity at different pH showed a maximum adsorption capacity in the pH range of 7–10. Lastly, we demonstrated that the DA beads are capable of slowly releasing most of the adsorbed phosphate, which is an important criterion for them to be an effective phosphorous fertilizer. This study, using DA composite hydrogel as an example, demonstrates a promising strategy of immobilizing ultrafine mineral adsorbents into biocompatible hydrogel matrix for effective recovery of phosphorous resource from wastewater.   © 2019 Water Environment Federation

• **Practitioner points**
- Integration of dolomite and alginate hydrogel beads is demonstrated using ball milling.
- Ball milling process increases the specific adsorption capacity of dolomite on phosphorus.
- Adsorption isotherms, kinetics, and pH effects of the dolomite–alginate beads are investigated.
- The dolomite–alginate beads can be used as slow-release phosphorus fertilizer.

• **Key words**
alginate hydrogel beads; ball mill; dolomite; phosphate absorption; slow-release fertilizer

INTRODUCTION

PHOSPHORUS (P) is an essential element for all forms of lives and a critical resource for modern agriculture that heavily depends on fertilizer. However, the current global supply of P relies heavily on mining of high quality phosphate minerals, making P an exhaustible resource (Cordell, Rosemarin, Schröder, & Smit, 2011). Indeed, a recent concept of "peak phosphorus" proposed that global supply of P will peak in foreseeable future (Déry & Anderson, 2007). On the other hand, there is a significant amount of P in domestic and agro-industrial wastewaters. Excessive discharge of P from wastewater into the aquatic ecosystem can cause algal boom and eutrophication (Conley et al., 2009). Thus, there are strong incentives to remove P from wastewaters and recover it as a valuable resource (Mayer et al., 2016).

Common techniques for removing P from wastewaters include precipitation by metal salts, microbial uptake, and assimilation into vegetation in constructed wetlands

(Cordell et al., 2011; Cornel & Schaum, 2009). While most of these approaches result in a solid waste with immobilized P, precipitation of P to form struvite ($MgNH_4PO_4 \cdot 6H_2O$) has been recently widely promoted as a means to recover P from wastewater for direct use as fertilizer (Etter, Tilley, Khadka, & Udert, 2011; Ishii & Boyer, 2015; Shu, Schneider, Jegatheesan, & Johnson, 2006). However, it is economically and operationally challenging to produce high content struvite from real wastewater due to the high cost of chemical dosage and the difficulty of small particle collection (Hao, Wang, van Loosdrecht, & Hu, 2013). Using adsorbents to remove and recover P from wastewater thus presents a promising alternative if an environmentally sustainable and economically viable adsorbent can be designed. To date, different types of natural minerals or synthetic adsorbents, such as iron oxide, palygorskite, magnetite, dolomite, and biochar, have been extensively tested for their P removal efficiency (Gan, Zhou, Wang, Du, & Chen, 2009; Karaca, Gürses, Ejder, & Açıkyıldız, 2006; Rashid, Price, Gracia Pinilla, & O'Shea, 2017; Shepherd, Sohi, & Heal, 2016; Suresh Kumar et al., 2017; Wan, Wang, Li, & Gao, 2017; Wang, Chen, Yu, Hu, & Feng, 2016; Yao, Gao, Chen, & Yang, 2013; Yuan et al., 2015).

In general, adsorbents are used in granular or powder forms, each with advantages and disadvantages. Granular adsorbents are easy to be separated and/or regenerated. However, because mineral adsorbents usually do not have micro-porosity as in activated carbon, the large size of granular adsorbent inevitably results in a lower specific surface area, which leads to a low specific adsorption capacity (SAC), defined as the amount of adsorbate (P in this case) removed by a unit mass of adsorbent. Powder adsorbents have relatively small particle sizes and offer significantly large specific surface area, which consequently leads to a high SAC. However, due to their poor hydraulic properties, removing fine power adsorbents from the treated water requires extra unit processes such as coagulation–flocculation–sedimentation or membrane filtration, which adds additional cost to the treatment process. The separation of powder adsorbents becomes even more challenging if submicron or even nanoscale adsorbents with ultrahigh specific area are to be used. Microfiltration or even ultrafiltration may have to be employed for separating the ultrafine adsorbents.

A promising solution to harness the very high SAC of fine powder adsorbent without costly post-separation is to immobilize the adsorbents into macroscopic matrices. This approach has been employed in previous studies to incorporate nanomaterials for various applications (Lin et al., 2013; Wang, Liu, Wang, & Yang, 2016; Zhao et al., 2015). For example, silver nanoparticles were immobilized in cross-linked alginate beads of millimeter sizes (when hydrated) for packed-column disinfection (Lin et al., 2013). Alginate hydrogel, a biocompatible and biodegradable material, is a highly porous and hydrated matrix that allows fast ion transport. The integration of nanoscale silver nanoparticles in a low-cost alginate hydrogel matrix maximized the utility of silver nanoparticles while eliminating the need to recover these particles from the disinfected water. A similar approach can be employed to prepare hydrogel-based composite adsorbent integrated with ultrafine active P absorbent materials to take advantage of the SAC of the active adsorbent materials. If the hydrogel is readily biodegradable and adsorbent material is agriculturally compatible, the composite matrix with adsorbed P can be directly applied as fertilizer.

In this study, we demonstrate the effectiveness of this approach using dolomite as the active adsorbent material. Dolomite, $CaMg(CO_3)_2$, is an abundant natural carbonate mineral and a commonly used soil conditioner for pH adjustment (Krauskopf & Bird, 1995). Previous studies have shown that dolomite particles can effectively remove phosphate from wastewater (Karaca et al., 2006; Yuan et al., 2015). However, commonly available dolomite has a relatively low adsorption capacity, while its small size (from tens to hundreds of microns) makes it hard to remove from the suspension. Herein, we use calcium cross-linked alginate as the porous hydrogel matrix to incorporate ultrafine dolomite particles obtained using ball milling. Experiments are conducted to establish the adsorption isotherms and quantify the adsorption kinetics. We further study the impact of pH on equilibrium adsorption capacity. Finally, we also conduct experiments to assess the kinetics of P release from the dolomite–alginate matrix, as controlled release is an important requirement for fertilizer application.

Experimental Section

Materials
Dolomite powder was obtained from Greenway Biotech Inc. Sodium alginate, L-ascorbic acid, calcium chloride ($CaCl_2$, Sigma-Aldrich, St. Louis, MO), ammonium molybdate (VI) tetrahydrate (($NH_4)_6Mo_7O_{24} \cdot 4H_2O$, ACROS, Pittsburgh, PA), antimony potassium tartrate trihydrate ($K_2Sb_2(C_4H_2O_6)_2$ $3H_2O$, Alfa Aesar, Tewksbury, MA), sodium acetate (CH_3COONa), ammonium chloride (NH_4Cl), magnesium sulfate ($MgSO_4$), and potassium phosphate monobasic (KH_2PO_4; Fisher Chemical, Pittsburgh, PA) were all used as received without purification.

Preparation of dolomite–alginate (DA) hydrogel beads
A solution of 20 g/L alginate was first prepared by dissolving 1 g of sodium alginate in 50 ml of deionized (DI) water. Then, 10 ml of the alginate solution and 25, 50, 75, and 100 mg of dolomite powder were added into an agate milling jar with 60 g agate milling balls, respectively. Ball milling was performed using a planetary ball mill (DECO-PBM-V-0.4L, DECO equipment, China) at a rotation speed of 425 rpm and a revolution speed of 212 rpm for 3.5 hr. Among the four dolomite concentrations used, the 75 mg one resulted in the best slurry condition in terms of homogeneity under our experimental conditions. Therefore, we chose this dolomite concentration throughout our study. To prepare the DA hydrogel beads, the alginate–dolomite slurry obtained from ball milling was injected dropwise into a solution of 0.3 mole/L $CaCl_2$ at a flow rate of 3 ml/min controlled using a syringe pump. Spherical beads of calcium cross-linked hydrogel enmeshing ultrafine dolomite particles formed from the dolomite–alginate slurry mixture immediately upon contacting $CaCl_2$ solution. The resulting hydrogel beads were washed using DI water thoroughly and stored in DI water prior to use.

Characterization and analytical methods

Scanning electron microscopy (SEM) imaging of the pristine and ball-milled dolomite powders was conducted using a Zeiss Merlin SEM. Thermogravimetric analysis (TGA) was performed on an SDT Q600 thermal analyzer (TA Instrument, New Castle, DE) under N_2 atmosphere at 10°C/min. Surface area of the raw dolomite and ball-milled dolomite powders was measured using a gas sorption analyzer with Brunauer–Emmett–Teller (BET) model (Autosorb iQ, Quantachrome, Boynton Beach, FL). Phosphate concentration of solution samples from the sorption experiments (see below) was measured using the molybdenum-blue colorimetric method using an ultraviolet-visible (UV-Vis) spectrophotometer (Cary 60, Agilent, Santa Clara, CA) at 700 nm wavelength (Murphy & Riley, 1962). Standard calibration curve was obtained using KH_2PO_4 solutions with varied concentrations. To measure the surface potential of the dolomite powder, we first prepared a suspension of colloidal dolomite particles by sonicating dolomite powder in water. The zeta potential of the dolomite colloidal particles in the supernatant after sonication was determined by laser Doppler micro-electrophoresis using a Zetasizer (Malvern Nano ZS, UK).

Batch adsorption experiments

In batch adsorption experiments, the dolomite–alginate (DA) beads containing 45 mg dolomite were added into 50 ml of KH_2PO_4 solution in sealed flasks reactors. These reactors were constantly stirred using a shaker at 250 rpm in an incubator at three different temperatures (20, 30, and 40°C) for 3 hr for the adsorption to reach equilibrium. The concentration of phosphate (in terms of mass concentration of elementary P) ranged from 5 to 100 mg/L, with the pH of the solution adjusted to 6.5. Synthetic wastewater was also tested in adsorption experiments. The synthetic wastewater was prepared using 0.64 g/L CH_3COONa, 57 mg/L NH_4Cl, 11.5 mg/L $CaCl_2$, 12 mg/L $MgSO_4$, and KH_2PO_4 with target concentration. Adsorption isotherms were evaluated using four different models, including Langmuir, Freundlich, Langmuir–Freundlich, and Redlich–Peterson models (Supporting Information Table S1) to identify the best fitting. Adsorption kinetics were evaluated using pseudo-first-order and pseudo-second-order models.

Phosphate release experiment

After 3-hr batch sorption experiments, phosphate-loaded DA beads were collected and dried at 100°C to prepare DA dry beads. The drying process significantly reduced the size and mass of the DA beads. In phosphate release experiments, 0.1 g of the dried DA beads was added into 50 ml DI water in a sealed flask. The flask was then constantly stirred at 250 rpm with a shaker in an incubator at 20°C. Five milliliter of the liquid sample was taken out from the flask every 24 hr for phosphate concentration measurement. The water volume was always maintained at 50 ml by replenishing the flask with 5 ml of DI water every time after sampling the solution. The cumulative release of phosphate was quantified using results from the release experiments and compared to the total amount of phosphate adsorbed by the DA beads calculated from batch adsorption experiments.

RESULTS AND DISCUSSION

Properties of the DA composite beads

The dolomite powder before ball milling was highly heterogeneous in size, with particle size ranging from a few to 300 microns (Figure 1a). These larger particles were poorly dispersed in water and could not form a homogeneous mixture with the alginate solution to prepare alginate–dolomite slurry.
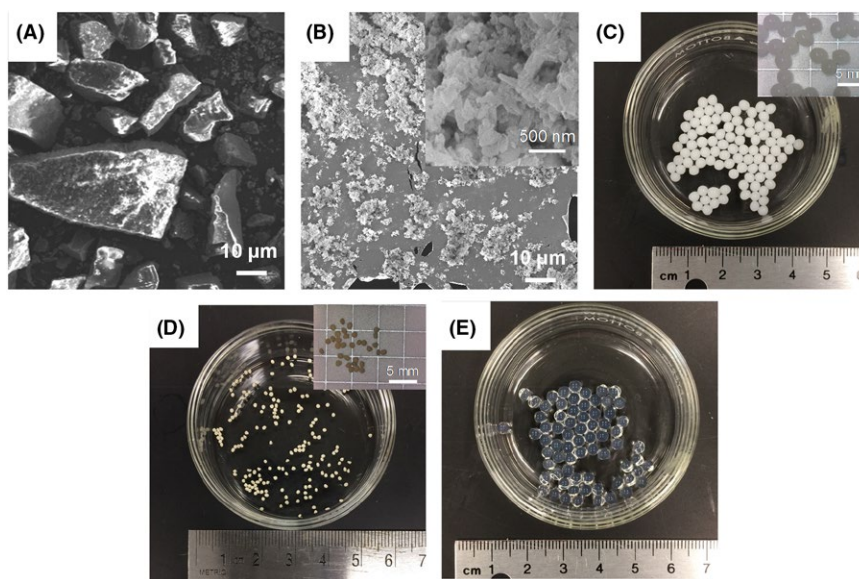

Figure 1. SEM images of dolomite powders (a) before and (b) after ball milling. Photographs of (c) wet DA beads and (d) fully air-dried DA beads, and (e) wet blank alginate beads, respectively.

Ball milling reduced the particle size and drastically increased the specific surface area as the particles appeared to become highly dendritic (Figure 1b). The BET surface area of dolomite increased from 3.08 to 40.79 m²/g after ball milling because of the decrease of particle size. It is difficult to accurately quantify the particle size distribution because of the strong and evident size heterogeneity. In addition, the micron-sized particles after ball milling are large aggregates of much smaller nanoscale particles (Figure 1b), whereas the pristine dolomite particles before ball milling have clear crystal structure (Figure 1a). Analysis of the photographic images of the as-prepared, hydrated DA beads and the fully air-dried DA beads suggest that their diameters are 2.76 ± 0.35 and 1.15 ± 0.10 mm, respectively (Figures 1c,d). The successful integration of dolomite particles is evident by comparing the color of DA beads (Figure 1c) and that of the calcium cross-linked blank alginate beads without dolomite (Figure 1e). Specifically, the DA beads are white and opaque, whereas the blank alginate beads are translucent.

More quantitative analysis of the DA bead composition is given by TGA. TGA curves of raw dolomite (without alginate) showed noticeable weight loss in the temperature range from 600 to 810°C, which can be attributed to single stage decomposition (Figure 2a; Valverde, Perejon, Medina, & Perez-Maqueda, 2015):

$$CaMg(CO_3)_2 \rightarrow CaO + MgO + 2CO_2(g).$$
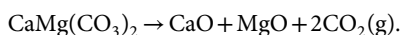
For the hydrated alginate beads without dolomite, about 95% weight was lost below 125°C due to the loss of water in hydrogel (Figure 2b). Calcium alginate itself started to decompose at about 200°C, where two decomposition stages were

observed (Figure 2b,c). The weight loss in first stage (200–300°C) is attributed to the degradation of the carboxyl group, as CO_2 is released. The second stage occurred in the range of about 400–550°C and is attributed to the degradation of polymer chain (Liang & Hirabayashi, 1992; Sun et al., 2012). Predried DA sample showed a combined TGA feature of dolomite and alginate, indicating that their thermal decomposition behavior remained unchanged. For the hydrated DA beads, TGA results showed that the sample contained about 93% of water, which is slightly less than that of the alginate hydrogel without dolomite integration. Based on the weight loss rates of the dolomite and the alginate beads, the dry mass ratio of alginate gel and dolomite is estimated to be about 1.9:1.

Adsorption isotherms

The isotherms for phosphate adsorption onto DA beads at three different temperatures are shown in Figure 3 for experiments conducted with phosphate solution (Figure 3a) and synthetic wastewater (Figure 3b). The experimental results were fitted with four different adsorption isotherm models with the detailed fitting parameters for each model listed in Supporting Information Tables S1 and S2. Among all four models attempted, the Langmuir–Freundlich model provided the best overall fitting with the minimum average coefficient. The better fitting power of the Langmuir–Freundlich model is not surprising though, as the model has one extra parameter than the Langmuir or Freundlich model. The applicability of a more complex empirical adsorption model suggests that phosphate adsorption onto dolomite is not just a simple monolayer adsorption process, but rather a complex process involving possible formation of surface precipitates such as calcium phosphate minerals (Xu et al., 2014).
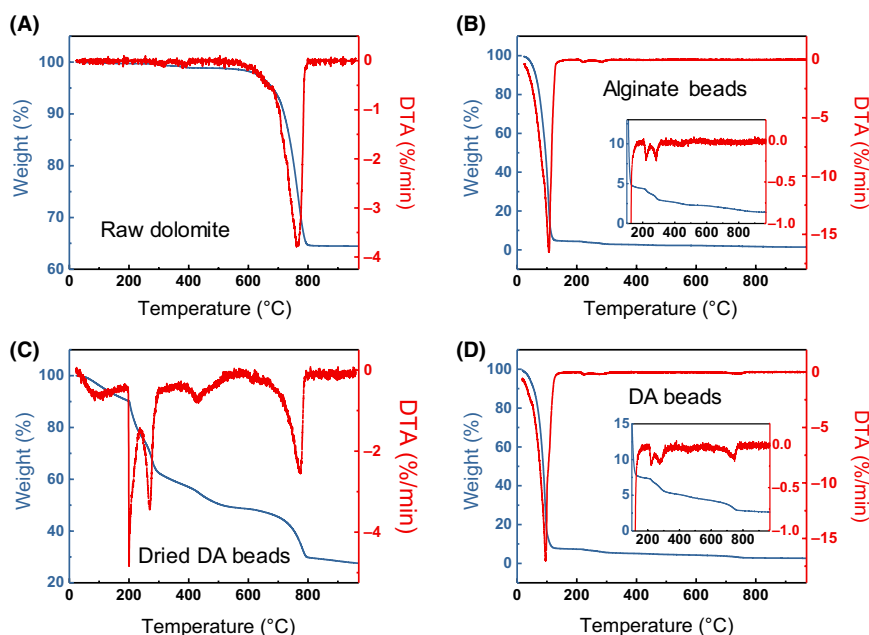

Figure 2. TGA-DTA analyses for the (a) raw dolomite powders, (b) alginate hydrogel beads, (c) air-dried DA beads, and (d) DA hydrogel beads. Analyses were conducted under pure N₂ at 10°C/min. The insets of (b) and (d) show the enlarged TGA curves after 100°C.
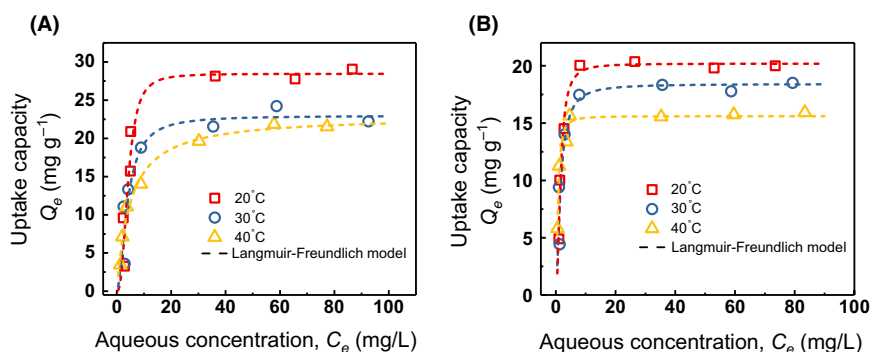
Figure 3. Adsorption isotherms of phosphate with (a) pure phosphate solution and (b) synthetic wastewater. The mass concentrations of P species in both equilibrium adsorption capacity (Q_e) and equilibrium aqueous concentration (C_e) are reported using the mass of P (instead of phosphate). Dash lines are the fitted Langmuir–Freundlich isotherms.

Based on the Langmuir–Freundlich model, the specific adsorption capacity (SAC) measured using phosphate solution decreased from 28.45 mg/g at 20°C to 22.93 mg/g at 40°C, which suggests that phosphate adsorption is an exothermic process. Control experiments using calcium cross-linked alginate hydrogel beads without dolomite were also conducted, yielding an SAC of 1.26, 1.22, and 1.07 mg/g at 20, 30, and 40°C, respectively. The very low baseline SAC with dolomite-free alginate confirms that most of the phosphate adsorption capacity was contributed by the integrated dolomite and not from the alginate matrix itself. In addition, previous studies have reported significantly lower SAC of dolomite ranging from 4 to 15 mg/g (note that here we adopt a unit of mg *phosphorus* per gram of adsorbent, whereas some results reported in literature used mg *phosphate* per gram of adsorbent; Karaca et al., 2006; Xu et al., 2014; Yuan et al., 2015). In our study, the SAC of the pristine dolomite was measured to be 9.75 mg/g at 20°C, which is similar to previous reports using dolomite as the adsorbent, and is comparable to other minerals such palygorskite clay or hematite (Dimirkou, Ioannou, & Doula, 2002; Gan et al., 2009). The much higher SAC achieved with our composite DA beads is attributable to the smaller particle size of the ball-milled dolomite and the much larger surface area available for phosphate adsorption.

Adsorption isotherms were also measured using synthetic wastewater to investigate the performance of the DA beads

in more practical environmental conditions (Figure 3b). The Langmuir–Freundlich model again provides the best fit to the results (Supporting Information Table S3). In the presence of competing ions, the SAC decreased from 28.45 to 20.19 mg/g at 20°C. Nevertheless, the DA beads still exhibited significantly higher SAC compared to that of pristine dolomite particles, which confirms the strong potential of enhancing SAC by immobilizing fine adsorbents using hydrogel for phosphate removal in practice.

Adsorption kinetics

The kinetics of phosphate uptake was investigated by measuring the time-dependent SAC of the DA beads with both pure phosphate solution (Figure 4a) and synthetic wastewater (Figure 4b). All the time-dependent SAC curves are best fitted with a pseudo-first-order model (Supporting Information Table S4), which suggests that the adsorption is diffusion controlled in our DA composite system (Simonin, 2016). Previous studies using dolomite as the adsorbent have shown pseudo-second order adsorption kinetics, which suggests the binding of the molecules onto the adsorbent surface to be the rate-limiting step, that is, the adsorption onto dolomite was reaction-limited (Yuan et al., 2015).

In our system, the ultrafine dolomite particles were embedded in the DA beads of an average diameter of 2.7 mm.
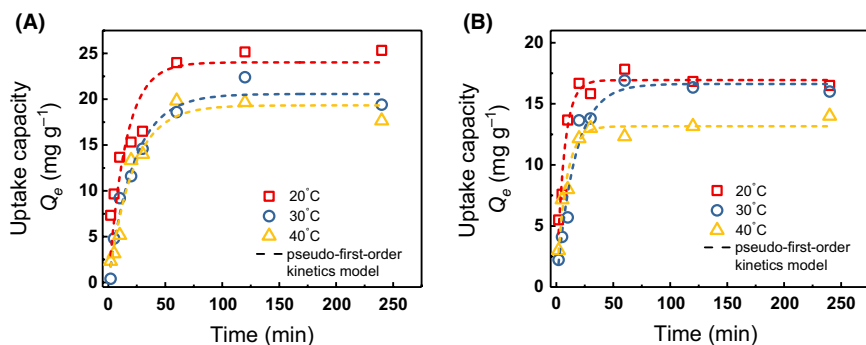

Figure 4. Adsorption kinetics of phosphate in (a) pure phosphate solution and (b) synthetic wastewater at pH 6.5 ± 0.1. Starting P concentration was 50 mg/L. Dash lines are fitted data using pseudo-first-order kinetics model.

Compared to the dolomite-only system as in previous studies (where dolomite particles were in direct contact with phosphate ions), the DA beads require a larger mean diffusion distance for phosphate adsorption. In other words, phosphate ions need to diffuse a longer distance before they can reach the adsorption sites on the dolomite particles inside the DA matrix. This difference in mean diffusion distance can explain the different kinetic characteristics observed in this study and in previous studies. Nevertheless, the phosphate adsorption rates with the DA beads shown in Figure 4 are still comparable to previously reported values for dolomite-only systems.

pH-dependence of maximum adsorption capacity

Aqueous phosphate has multiple species depending on solution pH, including phosphoric acid (H_3PO_4), dihydrogen phosphate ($H_2PO_4^-$), hydrogen phosphate (HPO_4^{2-}), and phosphate (PO_4^{3-}). Because the interaction between different phosphate species and the dolomite surface strongly depends on pH, we conducted a series of experiments to quantify the maximum SAC of the DA beads for total phosphate adsorption at different pH. The experimental results suggest that total phosphate adsorption by the DA beads was most efficient in the pH range between 7 and 10, at which the dominant phosphate species is HPO_4^{2-}. The SAC for total phosphate was 35.0 and 38.3 mg/g for pH 7 and 10, respectively (Figure 5a).

Zeta potential measurement of dolomite colloidal particles suggests that the surface of dolomite is consistently negatively charged at pH above 4 (Figure 5b). It is thus unlikely that the enhanced phosphate adsorption at pH 7–10 was due to stronger electrostatic attraction with the more negatively charged HPO_4^{2-} as compared to HPO_4^-. Therefore, the removal of phosphate by dolomite may involve more complex processes than simple binding of phosphate species onto available sites on the dolomite surface. It has been proposed by previous studies that phosphate adsorption onto dolomite surface may involve interfacial dissolution of Ca^{2+} and Mg^{2+} and consequent precipitation of Ca and/or Mg solid phase(s) (Xu et al., 2014). In low pH range (2–6), the predominant phosphate species is $H_2PO_4^-$. However, since the solubility of $Ca(H_2PO_4)_2$ is relatively high, the phosphate uptake capacity is compromised by the difficulty to form phosphate precipitate near the dolomite surface. When the pH is above 10, there are two possible mechanisms for the reduced surface uptake of phosphate. First, the dominant form of phosphate in this pH range is PO_4^{3-}. The high negative charge of PO_4^{3-} compared to its more protonated forms further reduces its concentration in the electrical double layer (EDL) emanating from a negatively charged dolomite surface. Second, a higher pH also inhibits the dissolution of Ca^{2+} and Mg^{2+} from dolomite and thus reduces their concentrations in the EDL. Both mechanisms synergistically reduce the saturation index in the EDL and thus hinders the formation of interfacial phosphate precipitate.

Slow release of phosphate from DA composite beads

To test the feasibility of using the DA beads as a P fertilizer, experiments were performed to evaluate the rate of P release from the DA beads to aqueous solution. Slow release has the benefit of maximizing the utilization of P, especially when
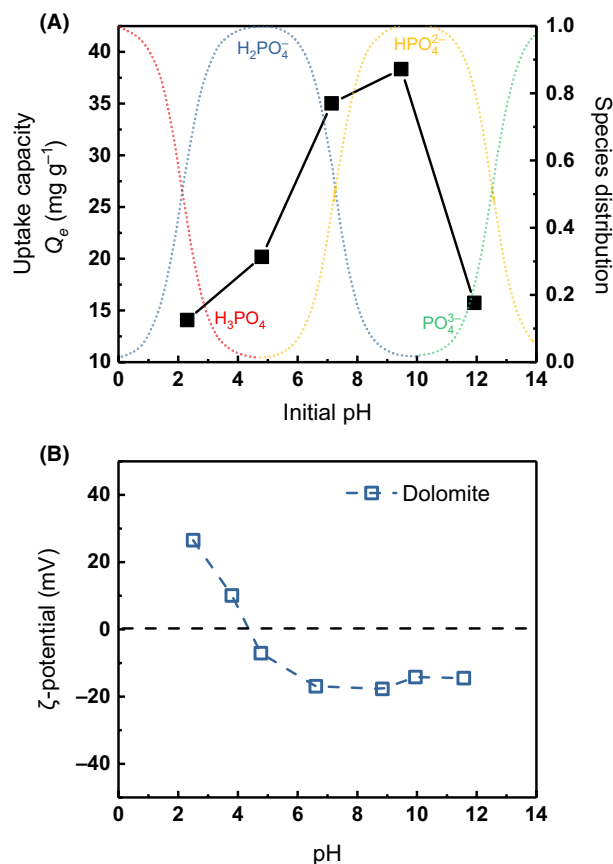
Figure 5. (a) Distribution of phosphate species as a function of solution pH and the effect of initial solution pH on the adsorption of phosphate at 20°C. (b) Zeta potential of the dolomite colloidal particles.

the fertilizer is applied to soil, because more soluble forms of P fertilizer are susceptible to soil runoff (Rashidzadeh & Olad, 2014; Zhan, Liu, Guo, & Wu, 2004). The samples used in the release experiments were phosphate-saturated DA beads obtained in the batch adsorption experiment after 3 hr of adsorption that leads to a saturated specific phosphate uptake capacity of 28 mg/g. As discussed above, phosphate is likely adsorbed onto the dolomite surface both as surface complexed species and calcium/magnesium phosphate precipitates. Because these precipitates typically have low solubilities, phosphate release will be a slow process controlled by the precipitation equilibrium. Therefore, the DA beads can be considered as a slow-release fertilizer (Shaviv & Mikkelsen, 1993). It should be noted that the phosphate release rate here is also affected by the sampling and water replenish process. As Figure 6 shows, about 90% of the adsorbed phosphate was released over a 60-day period, suggesting that most adsorbed phosphate can be gradually released for utilization as fertilizer. More specifically, phosphate release was relatively fast in the first 10 days in which about 40% of the phosphate had been released.

We note that when added into the water, the dried DA beads were subject to a small degree of swelling, but did not recover to
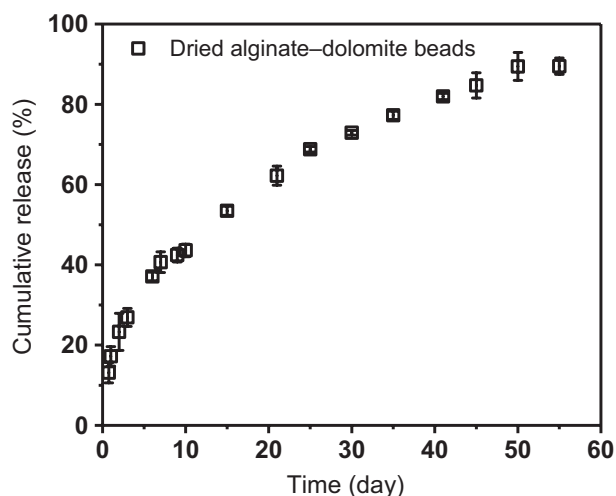
Figure 6. Cumulative percentage of phosphate release from the phosphate-saturated DA beads in DI water at 20°C.

their original size before drying. This phenomenon indicates that the structural change of the hydrogel is partially irreversible. The compact matrix structure of the DA beads after drying further slows down phosphate release, likely due to the lower in-matrix diffusion rate as a result of smaller porosity. The above result demonstrates that the DA beads with adsorbed phosphate can potentially serve as a promising slow-release P fertilizer.

CONCLUSIONS

Dolomite-alginate hydrogel beads were successfully prepared, integrating ultrafine dolomite particles with large surface area into a low-cost, natural, and biodegradable matrix of calcium cross-linked alginate. Adsorption isotherms showed that the phosphate uptake by the DA beads followed the Langmuir–Freundlich adsorption isotherm, indicating the presence of complex surface adsorption phenomena. Pseudo-first-order adsorption kinetics was observed, suggesting that the adsorption was diffusion controlled. In addition, adsorption experiments over a wide range of pH showed that maximum adsorption capacity was achieved at pH 7–10. Finally, phosphorus release experiments demonstrate the ability of the dry phosphate-loaded DA beads to release most of the adsorbed phosphate to water over a relatively long period of time, which is a key characteristic required for the phosphate-saturated DA beads to be used as fertilizer. Since both alginate and dolomite are low-cost, abundant, and agriculturally compatible materials, the results from this study demonstrate that the prepared DA beads can be a promising material not only for phosphate recovery, but also served as a slow-release phosphate fertilizer.

While the reported study uses dolomite as the adsorbent and alginate as the carrying matrix for demonstration, such an approach of using biodegradable hydrogel as the carrying matrix can be applied to integrate many different types of micron or nanoscale adsorbents. The same matrix can also host multiple types of adsorbents to achieve multi-functional adsorption.

Previous studies using nanoscale adsorbents have shown very strong application potential due to their huge specific area. However, the practical applications of nanoscale adsorbents have been limited by the difficulty or high cost of post-adsorption separation. The approach of hydrogel integration reported in this study is promising in overcoming this challenge and facilitate the practical adoption of nanoscale high-performance adsorbents for large scale practical applications.

CONFLICT OF INTEREST

The authors declare no conflict of interest.

REFERENCES

Conley, D. J., Paerl, H. W., Howarth, R. W., Boesch, D. F., Seitzinger, S. P., Havens, K. E., … Likens, G. E. (2009). Controlling eutrophication: Nitrogen and phosphorus. *Science*, *323*(5917), 1014. https://doi.org/10.1126/science.1167755

Cordell, D., Rosemarin, A., Schröder, J. J., & Smit, A. L. (2011). Towards global phosphorus security: A systems framework for phosphorus recovery and reuse options. *Chemosphere*, *84*(6), 747–758. https://doi.org/10.1016/j.chemosphere.2011.02.032

Cornel, P., & Schaum, C. (2009). Phosphorus recovery from wastewater: Needs, technologies and costs. *Water Science and Technology*, *59*(6), 1069. https://doi.org/10.2166/wst.2009.045

Déry, P., & Anderson, B. (2007). Peak phosphorus. *Energy Bulletin*.

Dimirkou, A., Ioannou, A., & Doula, M. (2002). Preparation, characterization and sorption properties for phosphates of hematite, bentonite and bentonite–hematite systems. *Advances in Colloid and Interface Science*, *97*(1), 37–61. https://doi.org/10.1016/S0001-8686(01)00046-X

Etter, B., Tilley, E., Khadka, R., & Udert, K. M. (2011). Low-cost struvite production using source-separated urine in Nepal. *Water Research*, *45*(2), 852–862. https://doi.org/10.1016/j.watres.2010.10.007

Gan, F., Zhou, J., Wang, H., Du, C., & Chen, X. (2009). Removal of phosphate from aqueous solution by thermally treated natural palygorskite. *Water Research*, *43*(11), 2907–2915. https://doi.org/10.1016/j.watres.2009.03.051

Hao, X., Wang, C., van Loosdrecht, M. C. M., & Hu, Y. (2013). Looking beyond struvite for P-recovery. *Environmental Science & Technology*, *47*(10), 4965–4966. https://doi.org/10.1021/es401140s

Ishii, S. K. L., & Boyer, T. H. (2015). Life cycle comparison of centralized wastewater treatment and urine source separation with struvite precipitation: Focus on urine nutrient management. *Water Research*, *79*, 88–103. https://doi.org/10.1016/j.watres.2015.04.010

Karaca, S., Gürses, A., Ejder, M., & Açıkyıldız, M. (2006). Adsorptive removal of phosphate from aqueous solutions using raw and calcinated dolomite. *Journal of Hazardous Materials*, *128*(2), 273–279. https://doi.org/10.1016/j.jhazmat.2005.08.003

Krauskopf, K. B., & Bird, D. K. (1995). *Introduction to geochemistry* (3rd ed.). New York, NY: McGraw-Hill.

Liang, C. X., & Hirabayashi, K. (1992). Improvements of the physical properties of fibroin membranes with sodium alginate. *Journal of Applied Polymer Science*, *45*(11), 1937–1943. https://doi.org/10.1002/app.1992.070451108

Lin, S., Huang, R., Cheng, Y., Liu, J., Lau, B. L. T., & Wiesner, M. R. (2013). Silver nanoparticle-alginate composite beads for point-of-use drinking water disinfection. *Water Research*, *47*(12), 3959–3965. https://doi.org/10.1016/j.watres.2012.09.005

Mayer, B. K., Baker, L. A., Boyer, T. H., Drechsel, P., Gifford, M., Hanjra, M. A., … Rittmann, B. E. (2016). Total value of phosphorus recovery. *Environmental Science & Technology*, *50*(13), 6606–6620. https://doi.org/10.1021/acs.est.6b01239

Murphy, J., & Riley, J. P. (1962). A modified single solution method for the determination of phosphate in natural waters. *Analytica Chimica Acta*, *27*, 31–36. https://doi.org/10.1016/S0003-2670(00)88444-5

Rashid, M., Price, N. T., Gracia Pinilla, M. Á., & O'Shea, K. E. (2017). Effective removal of phosphate from aqueous solution using humic acid coated magnetite nanoparticles. *Water Research*, *123*, 353–360. https://doi.org/10.1016/j.watres.2017.06.085

Rashidzadeh, A., & Olad, A. (2014). Slow-released NPK fertilizer encapsulated by NaAlg-g-poly(AA-co-AAm)/MMT superabsorbent nanocomposite. *Carbohydrate Polymers*, *114*, 269–278. https://doi.org/10.1016/j.carbpol.2014.08.010

Shaviv, A., & Mikkelsen, R. L. (1993). Controlled-release fertilizers to increase efficiency of nutrient use and minimize environmental degradation – A review. *Fertilizer Research*, *35*, 1–12. https://doi.org/10.1007/BF00750215

Shepherd, J. G., Sohi, S. P., & Heal, K. V. (2016). Optimising the recovery and re-use of phosphorus from wastewater effluent for sustainable fertiliser development. *Water Research*, *94*, 155–165. https://doi.org/10.1016/j.watres.2016.02.038

Shu, L., Schneider, P., Jegatheesan, V., & Johnson, J. (2006). An economic evaluation of phosphorus recovery as struvite from digester supernatant. *Bioresource Technology*, *97*(17), 2211–2216. https://doi.org/10.1016/j.biortech.2005.11.005

Simonin, J.-P. (2016). On the comparison of pseudo-first order and pseudo-second order rate laws in the modeling of adsorption kinetics. *Chemical Engineering Journal*, *300*, 254–263. https://doi.org/10.1016/j.cej.2016.04.079

Sun, J.-Y., Zhao, X., Illeperuma, W. R. K., Chaudhuri, O., Oh, K. H., Mooney, D. J., … Suo, Z. (2012). Highly stretchable and tough hydrogels. *Nature*, *489*, 133. https://doi.org/10.1038/nature11409

Suresh Kumar, P., Prot, T., Korving, L., Keesman, K. J., Dugulan, I., van Loosdrecht, M. C. M., & Witkamp, G.-J. (2017). Effect of pore size distribution on iron oxide coated granular activated carbons for phosphate adsorption – Importance of mesopores. *Chemical Engineering Journal*, *326*, 231–239. https://doi.org/10.1016/j.cej.2017.05.147

Valverde, J. M., Perejon, A., Medina, S., & Perez-Maqueda, L. A. (2015). Thermal decomposition of dolomite under CO_2: Insights from TGA and in situ XRD analysis. *Physical Chemistry Chemical Physics*, *17*(44), 30162–30176. https://doi.org/10.1039/C5CP05596B

Wan, S., Wang, S., Li, Y., & Gao, B. (2017). Functionalizing biochar with Mg–Al and Mg–Fe layered double hydroxides for removal of phosphate from aqueous solutions. *Journal of Industrial and Engineering Chemistry*, *47*, 246–253. https://doi.org/10.1016/j.jiec.2016.11.039

Wang, D., Chen, N., Yu, Y., Hu, W., & Feng, C. (2016). Investigation on the adsorption of phosphorus by Fe-loaded ceramic adsorbent. *Journal of Colloid and Interface Science*, *464*, 277–284. https://doi.org/10.1016/j.jcis.2015.11.039

Wang, Q., Liu, S., Wang, H., & Yang, Y. (2016). In situ pore-forming alginate hydrogel beads loaded with in situ formed nano-silver and their catalytic activity. *Physical Chemistry Chemical Physics*, *18*(18), 12610–12615. https://doi.org/10.1039/C6CP00872K

Xu, N., Chen, M., Zhou, K., Wang, Y., Yin, H., & Chen, Z. (2014). Retention of phosphorus on calcite and dolomite: Speciation and modeling. *RSC Advances*, *4*(66), 35205–35214. https://doi.org/10.1039/C4RA05461J

Yao, Y., Gao, B., Chen, J., & Yang, L. (2013). Engineered biochar reclaiming phosphate from aqueous solutions: Mechanisms and potential application as a slow-release fertilizer. *Environmental Science & Technology*, *47*(15), 8700–8708. https://doi.org/10.1021/es4012977

Yuan, X., Xia, W., An, J., Yin, J., Zhou, X., & Yang, W. (2015). Kinetic and thermodynamic studies on the phosphate adsorption removal by dolomite mineral. *Journal of Chemistry*, *2015*, 853105. https://doi.org/10.1155/2015/853105

Zhan, F., Liu, M., Guo, M., & Wu, L. (2004). Preparation of superabsorbent polymer with slow-release phosphate fertilizer. *Journal of Applied Polymer Science*, *92*(5), 3417–3421. https://doi.org/10.1002/app.20361

Zhao, X. H., Li, Q., Ma, X. M., Xiong, Z., Quan, F. Y., & Xia, Y. Z. (2015). Alginate fibers embedded with silver nanoparticles as efficient catalysts for reduction of 4-nitrophenol. *RSC Advances*, *5*(61), 49534–49540. https://doi.org/10.1039/C5RA07821K